Journal of Sound and Vibration (2001) **242**(1), 179–193
doi:10.1006/jsvi.2000.3321, available online at http://www.idealibrary.com on IDEAL®

LETTERS TO THE EDITOR

AN ANALYSIS OF MODAL DAMPING SOURCES IN A RECIPROCATING ENGINE

Y. WANG AND T. C. LIM

Department of Mechanical Engineering, 290 *Hardaway Hall*, *Box* 870276, *The University of Alabama*, *Tuscaloosa*, *AL* 35487, *U.S.A. E-mail*: *tlim@coe.eng.ua.edu*

(*Received* 25 *July* 2000, *and in final form* 11 *August* 2000)

1. INTRODUCTION

This communication examines the time-varying distributions of numerous modal damping sources commonly found in a reciprocating engine. The study extends the work presented in an earlier note by Wang and Lim [1], which predicted the overall torsional damping coefficients of a single-cylinder unit in terms of its absolute crank angle position. Even though the present study relies on the same fundamental concept of applying the vibratory energy balance equation in conjunction with both quasi-static and motoring single-cylinder engine experiments, a new set of analytical formulations is also devised to decompose the overall damping effect into its various primary constituents associated with the reciprocating, rocking and rotating parts of the engine. In addition, the basic approach utilizes the torsional vibration measurements of the complete and several partially assembled single-cylinder engine configurations unlike the earlier analysis that relies on the fully installed engine only.

There are numerous known sources of damping mechanisms in a reciprocating engine which can provide significant level of vibratory energy dissipations and contribute to the overall parasitic losses as well. Some of major contributors may include the frictional interfaces between the piston and fixed cylinder bore, cross-head and slide shoe wall, connecting rod and cross-head or crank pin, and crankshaft and main journal bearings. Their effects are generally quite critical to the system modal vibration response. Hence, it is highly desirable to gain a better understanding of the precise damping contributions from these different sources. To the knowledge of the authors, no known study have successfully quantified this phenomenon thoroughly, and thus the damping characteristic in question remains quite vague.

Previous work on global damping effect in reciprocating engines and the evolution of the damping models has been cited in the earlier note [1]. A review of the relevant literature [2–11] reveals conflicting conclusions and inadequate information from some of the proposed results. For instance, Shannon [4], Federn and Broed [5], and Draminsky [6] initially stipulated that the vibration damping effect from the piston is negligible. On the other hand, Eshleman [7] showed that the magnitude of torsional damping coefficient is significantly controlled by the frictional interface of the piston ring and thus affected by the type of lubrication used. Research investigation on vibration damping specifically due to the cross-head component is almost non-existent. The only one known was performed by Maciotta and Merlino [8] who did not actually find any significant difference in the

0022-460X/01/160179 + 15 $35.00/0

damping levels of two nearly identical engines with and without the cross-head design, and hence concluded that the damping contribution from it is small. In the case of the connecting rod, Shannon [4] was able to neglect its damping effect completely in one of his vibration studies, but in another contrasting study Draminsky [6] experimentally found significant damping level from the crank pin of the connecting rod. The finding by Draminsky was consistent with the calculation made by Valev [9], which predicted major engine vibration damping in the crank pin. However, in some the reciprocating engine vibration models proposed by Shannon [4], Draminsky [6] and Hafner [10], the main journal bearings were semi-empirically determined to be the main damping contributor. In addition, Draminsky [6] pointed out that the material damping in the crankshaft could be quite significant in some systems. This led Iwamoto and Wakabayashi [11] to perform a study that revealed the importance of material damping in crankshaft of certain large, low-speed engines.

From the above brief historical discussions, it is clear that the main characteristic of vibratory energy dissipation from the various parts of the reciprocating engine, which is essential in the control of resonance response, is not completely well understood. Additionally, the time-dependent contributions from the primary sources of damping mechanisms have not been quantified accurately. These issues are addressed in this communication experimentally and analytically for the case of a two-stroke single-cylinder engine set-up containing a piston, cross-head, connecting rod, crankshaft and main journal-bearing pair. The analysis is performed from the viewpoint of the lumped parameter torsional system model where only the angular degree-of-freedom (d.o.f.) of the rotating components is considered.

2. DAMPING SOURCES AND MODELING

Figure 1 depicts the six commonly known sources of vibration damping in a typical single-cylinder reciprocating engine unit with cross-head included. Each damping source is described by a localized viscous damping coefficient term denoted by the appropriate subscript: C_{P1} (piston–cylinder bore), C_{P2} (cross-head-slide shoe), C_{R1} (connecting rod–cross-head pin), C_{R2} (connecting rod–crank pin), C_k (main journal bearings), and C_h (crankshaft). The first five damping coefficients are essentially due to the effect of sliding contact friction in their respective structural interfaces, while C_h represents the internal material damping the crankshaft component. Other unstated secondary sources of damping are assumed negligible here.

Similar to the formerly proposed lumped parameter torsional vibration analysis [1] that led to a simple multi-d.o.f. linear time-invariant system, only the angular perturbation response of the engine about the drive shaft rotational axis is considered in this extension work. Based on this assumption, each individual damping term has to be expressed in an equivalent torsional damping form associated with the angular d.o.f. of the crankshaft nodal point. This concept also readily provides a direct comparison of the damping effects arising from the six different sources of interest on a more equal basis.

Consider the perturbations about the mean rigid-body translation displacement of the piston/cross-head piece $X(t)$ measured from the top dead center (TDC) position denoted by $x(t)$ and the swing angle of the connecting rod $\beta(t)$ relative to the cylinder axis given by $\gamma(t)$ as shown in Figure 2. Note that their geometrical relationships to the crank angle $\alpha(t) = \Omega t$ and the associated angular sinusoidal fluctuation $\varphi = \Phi \sin(\omega t - \varepsilon_v)$, where Φ is the amplitude of torsional vibration motion, ω is the frequency of excitation and ε_v is the relative phase lag, have been derived in the earlier note by Wang and Lim [1]. For reference,

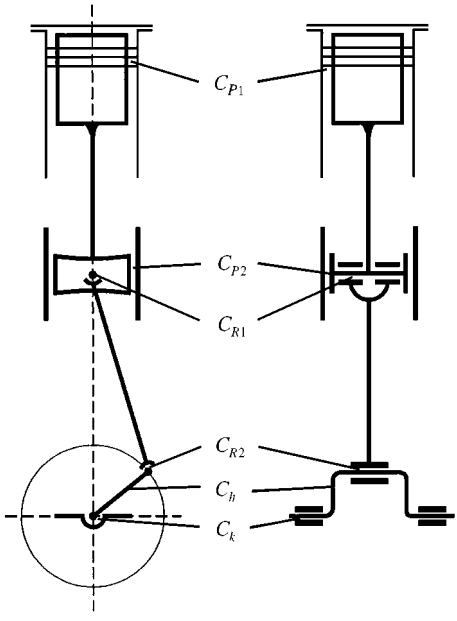

Figure 1. Damping sources in a typical single-cylinder reciprocating engine.

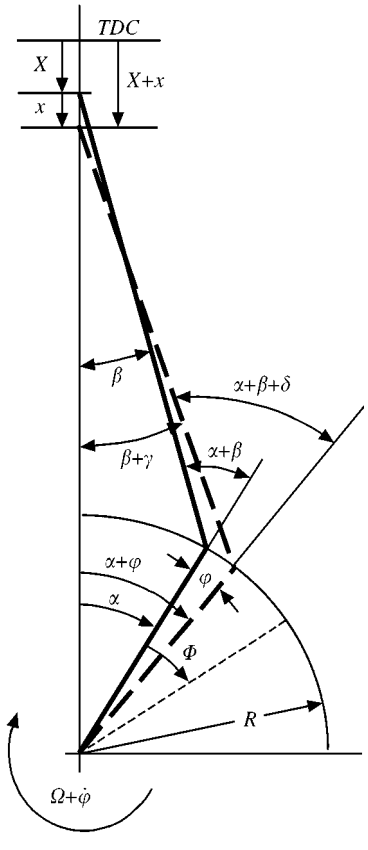

Figure 2. Perturbations in the translation and rotation motions of the reciprocating engine members.

the linearized perturbed velocities obtained from the time derivatives of the displacement terms are given by

$$\text{piston/cross-head:} \quad \dot{x} = R\dot{\varphi}[\sin(\alpha) + \lambda \sin(2\alpha)/2], \tag{1a}$$

$$\text{connecting rod:} \quad \dot{\gamma} = \dot{\varphi}[(\lambda + \lambda^3/8)\cos(\alpha) - \lambda^3 \cos(3\alpha)/8], \tag{1b}$$

where R is the crank radial distance and λ is ratio of R to the length of the connecting rod. The top expression in the above pair of equations relates directly to the level of vibratory energy dissipations between the piston and fixed cylinder bore, and cross-head and slide shoe wall, while the second term is associated with the level of vibration damping between the connecting rod and cross-head pin joint. Since our damping analysis will be performed over one complete vibration cycle, the rate of crank angular fluctuation can be expressed as $\dot{\varphi} = \omega\Phi\cos(\omega t)$ by letting $\varepsilon_v = 0$ without loss of generality. The above perturbation velocity terms in equation (1) then become

$$\text{piston/cross-head:} \quad \dot{x} = R[\sin(\alpha) + \lambda \sin(2\alpha)/2]\Phi\omega \cos(\omega t), \tag{2a}$$

$$\text{connecting rod:} \quad \dot{\gamma} = [(\lambda + \lambda^3/8)\cos(\alpha) - \lambda^3 \cos(3\alpha)/8]\Phi\omega \cos(\omega t). \tag{2b}$$

Similarly, the vibration energy dissipation between the crankshaft and crank pin joint can be related to the perturbation about the swing angle of the connecting rod relative to the crankshaft orientation, which is denoted by δ. Its corresponding perturbation velocity $\dot{\delta}(t)$ can be easily shown to be

$$\dot{\delta} = [1 + (\lambda + \lambda^3/8)\cos(\alpha) - \lambda^3 \cos(3\alpha)/8]\Phi\omega \cos(\omega t). \tag{3}$$

The total vibratory energy dissipation over a period of sinusoidal excitation due to translational and torsional viscous damping effects in the different sources discussed here can be generally formulated as

$$W = \int_{\omega t=0}^{\omega t=2\pi} [\underbrace{C_\varphi \dot{\varphi}\, \mathrm{d}\varphi}_{\text{(torsion)}} + \underbrace{C_x \dot{x}\, \mathrm{d}x}_{\text{(translational)}}], \tag{4}$$

where C_x and C_φ are the localized translation and torsional damping coefficients respectively. In this problem, C_{P1} and C_{P2} are translational types while C_{R1}, C_{R2}, C_k and C_h are torsional ones. Hence, the vibratory energy dissipations at each of the six sources in terms of α can be derived by substituting equations (2) and (3) into equation (4) and evaluating the integral over a period of ωt:

$$W_{\alpha P} = \pi\omega(C_{P1} + C_{P2})(R\Phi[\sin(\alpha) + \lambda \sin(2\alpha)/2])^2, \tag{5a}$$

$$W_{\alpha R1} = \pi\omega C_{R1}(r_1\Phi)^2[(\lambda + \lambda^3/8)\cos(\alpha) - \lambda^3 \cos(3\alpha)/8]^2, \tag{5b}$$

$$W_{\alpha R2} = \pi\omega C_{R2}(r_2\Phi)^2[1 + (\lambda + \lambda^3/8)\cos(\alpha) - \lambda^3 \cos(3\alpha)/8]^2, \tag{5c}$$

$$W_{\alpha c} = \pi\omega C_c(r_c\Phi)^2, \tag{5d}$$

where $C_c = C_k + C_h$, and r_1, r_2 and r_c are the radii of the upper and lower connecting rod pin joints, and main journal bearing respectively. Equating the first three equations above to an equivalent torsional vibration energy dissipation term associated with the rotational

co-ordinate of the drive shaft positioned at the base of the reciprocating engine, which is expressed as $\pi\omega C_\alpha \Phi^2$, yields the equivalent torsional viscous damping coefficients for the piston $C_{\alpha P1}$, cross-head $C_{\alpha P2}$, and connecting rod upper $C_{\alpha R1}$ and lower $C_{\alpha R2}$ pin joints as

$$C_{\alpha Pj} = C_{Pj} R^2 [\sin(\alpha) + \lambda \sin(2\alpha)/2]^2, \quad j = 1, 2, \tag{6a}$$

$$C_{\alpha R1} = C_{R1} r_1^2 [(\lambda + \lambda^3/8)\cos(\alpha) - \lambda^3 \cos(3\alpha)/8]^2, \tag{6b}$$

$$C_{\alpha R2} = C_{R2} r_2^2 [1 + (\lambda + \lambda^3/8)\cos(\alpha) - \lambda^3 \cos(3\alpha)/8]^2. \tag{6c}$$

Note that by definition C_c is already in the equivalent torsional form. Accordingly, the crankangle-dependent net-equivalent torsional damping coefficient examined in the earlier note [1] is given by

$$C_\alpha = C_{\alpha P1} + C_{\alpha P2} + C_{\alpha R1} + C_{\alpha R2} + C_c, \tag{7}$$

which clearly shows the decomposition of the net torsional damping term as a direct sum of its primary constituents.

The above torsional vibration damping coefficients are in fact time varying due to their dependency on $\alpha(t)$. The corresponding time-averaged torsional damping coefficients, assuming a steady state crankspeed, equals Ω and fundamental engine firing order of v can be derived by formulating the total torsional vibratory energy dissipation for one complete revolution of the crankshaft. The resulting time-averaged damping coefficient can be shown to be

$$C_Z = \frac{1}{2\pi} \int_0^{2\pi} C_\alpha [1 + \cos(2v\alpha)] \, \mathrm{d}\alpha. \tag{8}$$

It may be noted that for $v = 1$, the second term in the integral vanishes. Also, for $v \geqslant 3$, it is typically small compared to the first term that turns out to be identical to the average value of the damping coefficients within one crank cycle. Applying equation (8) to each term on the right-hand side of equation (7) yields another arithmetic sum of the individual time-averaged damping coefficients,

$$C_Z = C_{ZP1} + C_{ZP2} + C_{ZR1} + C_{ZR2} + C_c, \tag{9}$$

where the specific time-averaged torsional damping coefficients corresponding to the first four terms above are explicitly given by

$$C_{ZPj} = C_{Pj} R^2 (1 + \lambda^2/4)/2, \quad j = 1 \text{ or } 2, \tag{10a, b}$$

$$C_{ZR1} = \tfrac{1}{2} C_{R1} r_1^2 \lambda^2 (1 + \lambda^2/4 + \lambda^4/32), \tag{10c}$$

$$C_{ZR2} = \tfrac{1}{2} C_{R2} r_2^2 (2 + \lambda^2 + \lambda^4/4 + \lambda^6/32). \tag{10d}$$

Note that when the above equivalent torsional damping formulations represented by equations (6) and (7) or (9) and (10) are applied to the resonance points of the powertrain system, we can then obtain the corresponding instantaneous or time-averaged modal damping coefficients, respectively, which are the main interest of this study. Using a two-stroke single-cylinder reciprocating engine set-up developed in the previous analysis [1], these damping terms can be quantified by applying the vibratory energy balance equation. Furthermore, the summation superposition form of equations (7) and (9) suggests

a simple way to predict the equivalent torsional damping coefficients experimentally applying certain combinations of partially assembled engine configurations as discussed next.

3. EXPERIMENTAL RESULTS

The experimental powertrain set-up consisting of a single-cylinder engine system developed by the authors in an early study is utilized again here. Details of the test and measurement set-up are described in the earlier related paper [1]. The schematic of the powertrain layout and its corresponding engine parameters are given in Figure 3. Similar to the previous analysis, only the first two flexible system torsional modes between 28–33 and 78–88 Hz are examined in this study even though the theory is applicable to higher order modes as long as the assumed one-dimensional lumped parameter torsional system remains valid. The exact natural frequency depends on the orientation of the crank. Note that the first mode contains one nodal point while the second one contains two stationary points as described previously. Applying the vibratory energy balance condition at the system resonance where $\omega = \omega_p$ by equating the injected and dissipated power terms yields

$$\sum_{i=1}^{n} |T_i| \Phi_i = \sum_{i=1}^{n} C_i \omega_p \Phi_i^2 + \sum_{i=1}^{n-1} C_{i,i+1} \omega_p (\Phi_i - \Phi_{i+1})^2. \tag{11}$$

In the above expression, n is the total number of system co-ordinates, and $|T_i|$ and Φ_i are the externally applied harmonic torque fluctuation and amplitude of torsional response at point i. For the system shown in Figure 3, $n = 5$. In general, $|T_i|$ can be sensed experimentally or computed theoretically. The angular displacement vector $\{\Phi_i\}_p$ at resonance can be further expressed as $\{\Phi_i\}_p = \Phi_1 \{\Delta_i\}_p$, where $\{\Delta_i\}_p$ is the classically predicted mode shape vector corresponding to ω_p with $\Delta_1 = 1$. Making this substitution into equation (11), and solving for the absolute damping coefficient associated with the jth co-ordinate leads to

$$C_j = \frac{1}{\omega_p \Phi_1 \Delta_j^2} \sum_{i=1}^{n} |T_i| \Delta_i - \frac{1}{\Delta_j^2} \sum_{i=1, i \neq j}^{n} C_i \Delta_i^2 + \frac{1}{\Delta_j^2} \sum_{i=1}^{n-1} C_{i,i+1} (\Delta_i - \Delta_{i+1})^2, \tag{12}$$

where all terms on the right-hand side are measured or computed analytically and the jth co-ordinate represents the crankshaft d.o.f. Similar to the earlier paper [1], equation (12) is the fundamental expression used to predict the equivalent damping coefficient of the reciprocating engine. In order to determine the instantaneous and time-averaged damping coefficients using the proposed method, both quasi-stationary and operating tests are performed as outlined next.

First, let us consider the quasi-stationary experiments in which the exact nodal point between the flywheels 5 and 6 for the particular mode under consideration is physically constrained fixed. Clamping the appropriate points allows us to simulate the corresponding resonances when forced at their natural frequencies. In practice, this is achieved by using a pair of frequency sweeping, out-of-phase non-contacting magnetic exciters on the flywheel number 5 to seek out the exact point of resonance. To take advantage of the fact that the net-equivalent torsional damping is simply the sum of the individual damping terms associated with each one of the vibratory energy dissipation sources under consideration, three different test configurations are proposed. Clearly, one of configurations comprises of the complete engine installation like in the previous study [1]. This fully assembled set-up, labeled as 1A in Figure 3, provides the data used to predict the net damping coefficient C_α as

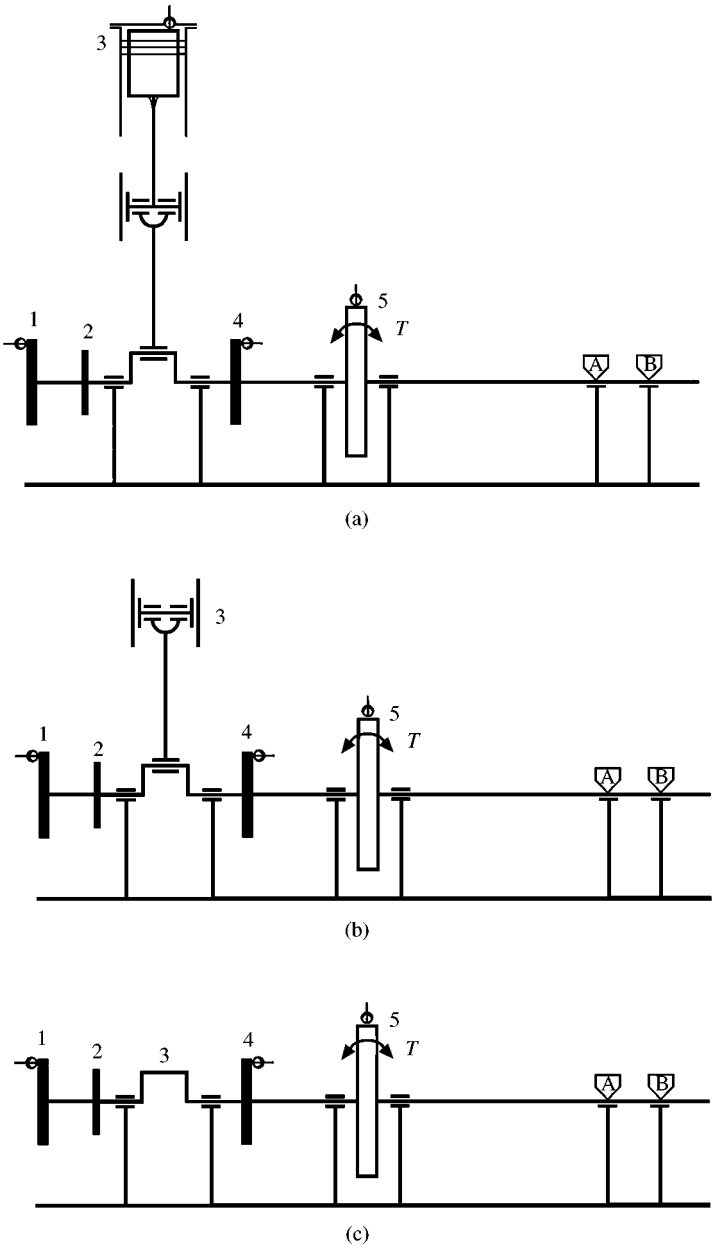

Figure 3. Proposed quasi-stationary experiments for prediction of time-varying modal damping coefficients of a single-cylinder engine with bore = 72 mm, stroke = 150 mm, $R = 75$ mm, $r_1 = 27{\cdot}5$ mm, $r_2 = 31$ mm and $\lambda = 0{\cdot}315$. Illustrated here are three different test configurations: (a) test 1A with complete engine installation; (b) test 1B with piston removed; (c) test 1C with crankshaft attached only. Lables: 1, measurement gear; 2, attachment disk; 3, cylinder; 4, measurement gear; 5, flywheel; (), accelerometers; (A), fixed nodal point for mode-1; (B), fixed nodal point for mode-2; (T), input torque fluctuation.

a function of crankangle. The second test set-up 1B is performed with the piston component removed from the engine installation, which produces the data used to compute the sum total of $(C_{\alpha P2} + C_{\alpha R1} + C_{\alpha R2} + C_c)$ in the absence of the piston damping effect. It should be clear that the difference between the results of tests 1A and 1B yields $C_{\alpha P1}$. Further, removal

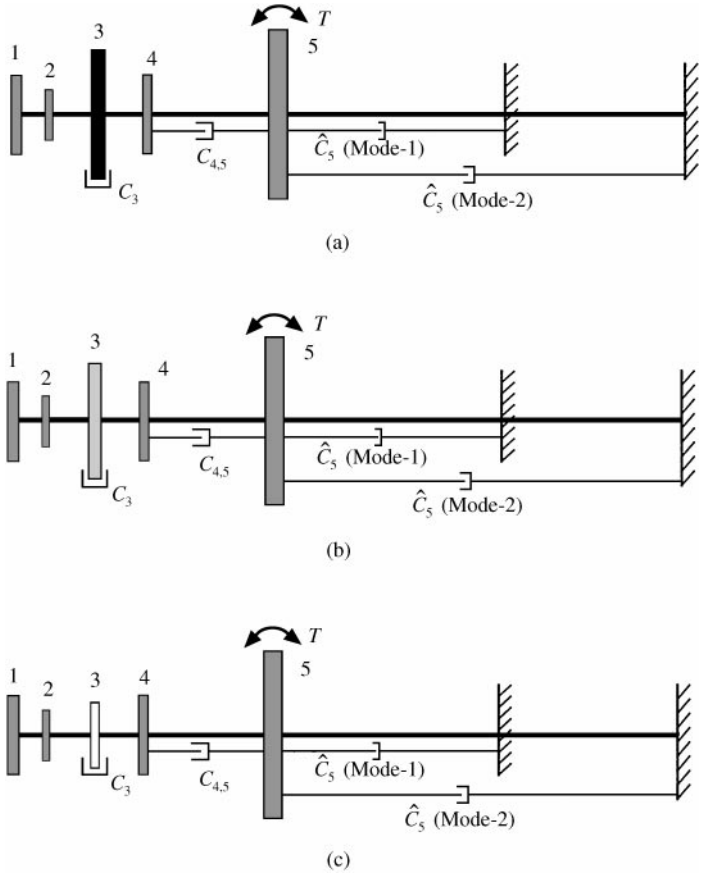

Figure 4. Lumped parameter torsional vibration models, expressed by $T_5\Delta_5 = \omega_p\Phi_1[C_3\Delta_3^2 + C_{4,5}(\Delta_4 - \Delta_5)^2 + \hat{C}_5(\Delta_5)^2]$, representing the proposed quasi-stationary experiments for prediction of crankangle-dependent modal damping coefficients: (a) complete engine torsional model; (b) engine torsional model without piston component; (c) engine torsional model with crankshaft attached only.

of the cross-head and connecting rod leads to the third test set-up 1C that directly gives C_c only. The corresponding lumped parameter torsional models for the three configurations analyzed as shown in Figure 4, where point 1 is the left most disk used in measuring Φ_1 and point $j = 3$ is the crankshaft location. Since the derivations of these mathematical models from the general form given by equations (11) and (12) are quite straightforward, the details will not be discussed here for brevity. For each case analyzed, the corresponding forms of vibratory energy balance equation as a function of only the non-zero coefficients are also noted in the figure. These experiments and calculations are repeated at every 15° increment of crankangle for one-half revolution to extract the instantaneous modal damping coefficient used to generate its inherent time-varying behavior.

Figure 5(a) shows the predicted composite modal damping coefficients associated with the crankshaft angular co-ordinate for the first two torsional modes using the quasi-stationary tests 1A and 1B. The familiar U-shape trend is again observed as reported by Wang and Lim [1]. Moreover, the predicted modal damping coefficient of mode 2 is always greater than that of the first mode, and the second test 1B without the piston generally provides lower modal damping coefficient as expected. The differences between

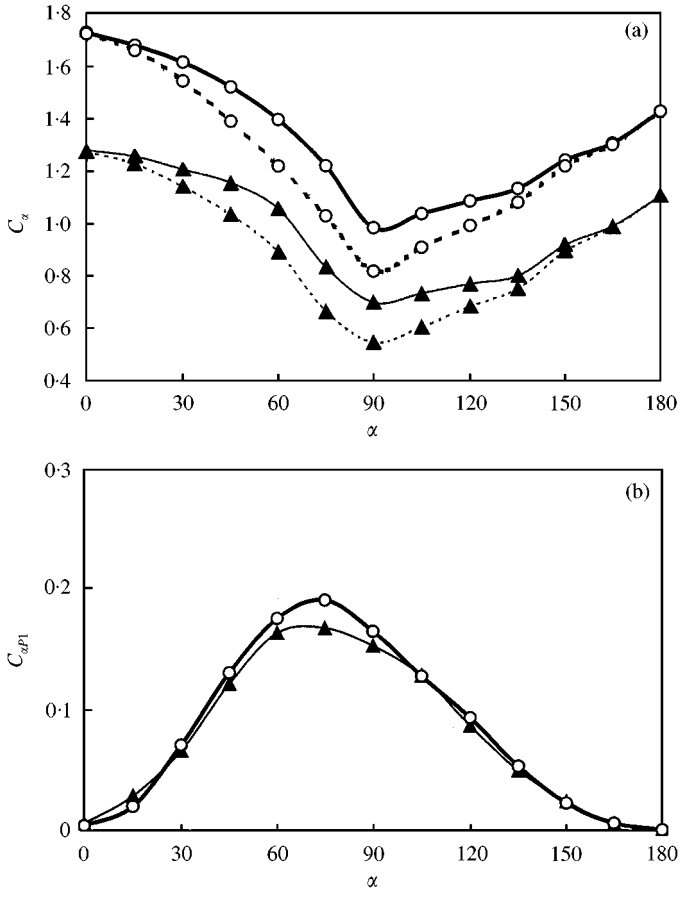

Figure 5. Predicted time-varying modal damping coefficients of modes 1 and 2 using a pair of quasi-stationary engine experiments: (a) composite modal damping coefficients derived from test 1A and 1B; (–○–), test 1A, mode-2; (···○···), test 1B, mode-2; (–▲–), test 1A, mode-1; (- -▲- -), test 1B, mode-1; (b) modal damping coefficients of piston cylinder bore; (–▲–), mode-1; (–○–), mode-2.

the damping results of the the two tests give the magnitudes of $C_{\alpha P1}$ for both modes 1 and 2 as shown in Figure 5(b). Again, the results show slightly higher modal damping in the second mode compared to the first mode even though the overall magnitudes are practically the same relative to the much larger net damping level in Figure 5(a). Note that the value peaks around 90° because the perturbation velocity of the piston $\dot{x}(t)$ is greatest at this point for the same level of input crank angular fluctuation $\dot{\varphi}(t)$. This fundamental difference in the trends compared to the net modal damping indirectly implies that the influence of $C_{\alpha P1}$ on vibration response at the resonance is not large. This effect can also be seen in Figure 6 that compares $C_{\alpha P1}$ to the rest of the modal damping coefficients.

With the exception of crankshaft modal damping C_c that is obtained directly from test 1C, the rest of the three modal damping coefficients presented in Figure 6 are determined using a least-squares regression method since it is physically not possible to separate the crosshead and connecting rod upper and lower pin joints using the proposed experimental set-up. Applying equation (7) to a series of α cases tested in 1A results in a set of linear algebraic equations. The total number of equations depends on the magnitude of the uniform crank angle interval used in the experimentation. For 15° increment, 13 separate

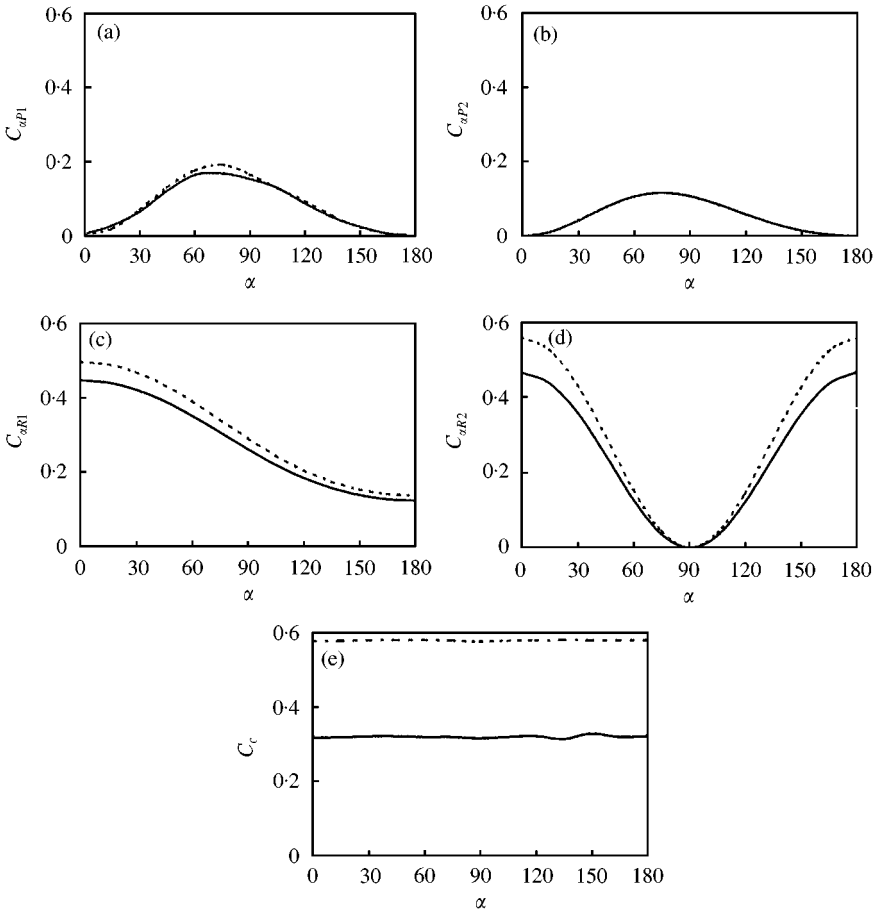

Figure 6. Modal damping contributions of the different vibratory energy dissipation sources: (a) piston–cylinder bore; (b) cross-head–slide shoe; (c) connecting rod–cross-head pin; (d) connecting rod–crank pin; (e) main journal bearings and crankshaft; (——), mode-1; (- - - - -), mode-2.

linear algebraic equations can be written

$$C_\alpha(\alpha) = C_{\alpha P1} + C_{\alpha P2} + C_{\alpha R1} + C_{\alpha R2} + C_c, \quad \alpha = 0, 15, 30, \ldots, 180^\circ, \tag{13}$$

where C_α, $C_{\alpha P1}$ and C_c are already known from earlier calculations, and $C_{\alpha P2}$, $C_{\alpha R1}$ and $C_{\alpha R2}$ are yet to be determined. Substitution of equation (6) that relates $C_{\alpha P2}$, $C_{\alpha R1}$ and $C_{\alpha R2}$ to the corresponding localized viscous damping coefficient terms into equation (13) leaves only a total of three unknown constants. Grouping the known and unknown damping coefficient terms into separate sides of the equality yields a rectangular matrix equation in the form of

$$[U_{k1}(\alpha_k)]_{13\times 3}\begin{Bmatrix} C_{P2} \\ C_{R1} \\ C_{R2} \end{Bmatrix}_{3\times 1} = \begin{Bmatrix} (C_{\alpha_1} - C_{\alpha_1 P1} - C_c) \\ (C_{\alpha_2} - C_{\alpha_2 P1} - C_c) \\ \vdots \end{Bmatrix}_{13\times 1}, \tag{14}$$

where U_{k1}, U_{k2} and U_{k3} are the coefficient multipliers for C_{P2}, C_{R1} and C_{R2} respectively. They are explicitly given by the right-hand side expressions of equations (6a–c).

TABLE 1

Direct and least-squares regression predictions of the time-invariant localized viscous damping coefficients (N s/m)

Parameters	Method	Mode 1	Mode 2
C_{P1}	Direct	0·2907	0·3122
C_{P2}	Least squares	0·1899	0·1895
C_{R1}	Least squares	15·4876	18·6215
C_{R2}	Least squares	0·6735	0·7487

Premultiplying equation (14) by the transpose of $[U]$ and solving for $\{C_{P2}, C_{R1}, C_{R2}\}^{\mathrm{T}}$ results in

$$\begin{Bmatrix} C_{P2} \\ C_{R1} \\ C_{R2} \end{Bmatrix}_{3\times 1} = ([U_{lk}(\alpha_k)]_{3\times 13}[U_{kl}(\alpha_k)]_{13\times 3})^{-1}[U_{k1}(\alpha_k)]_{3\times 13}\begin{Bmatrix} (C_{\alpha_1} - C_{\alpha_1 P1} - C_c) \\ (C_{\alpha_2} - C_{\alpha_2 P1} - C_c) \\ \vdots \end{Bmatrix}_{13\times 1}. \tag{15}$$

Applying this least-squares solution to the results of test 1A given in Figure 5(a) produces the numerical answers in Table 1. Then, the α-dependent results in Figure 6 are obtained by inserting these localized viscous damping coefficients back into equation (6). For α near 0 and 180°, the net modal damping coefficients given by Figure 5(a) are mostly dominated by connecting rod pin joints, and crankshaft/journal-bearing components. Also, because C_c is nearly independent of α, it continues to dominate the overall vibratory energy dissipation throughout the entire crankcycle. The modal damping coefficients of the piston and crosshead reach a maximum slightly below $\alpha = 90°$ but still less than the damping effect from the crankshaft/journal bearings and connecting rod upper pin joint. This finding directly confirmed the earlier analysis by Wang and Lim [1] that indirectly points to the crank-connecting rod interface areas as the dominant source of modal vibration damping in the reciprocating engine as opposed to the reciprocating piston/cross-head components.

The same engine set-up is also used to perform a series of running experiments as shown in Figure 7 to predict the time-averaged modal damping coefficients. The setups (labelled as 2A, 2B and 2C) are essentially the same as the ones tested in the quasi-stationary condition except for the motor component attached. Note that the motor damping coefficient C_8 was previously determined to be 1·6136 N m s/rad [1]. The equivalent lumped parameter torsional vibration models for these test cases are illustrated in Figure 8 along with the specific vibratory energy balance equations. The harmonic excitations in the first two tests are provided by the reciprocating engine components, which was classically shown by Den Hartog [2] and succesfully used by Wang and Lim [1]. In the third test 2C, the universal joint is misaligned slightly to incite a torsion excitation at the second harmonic of shaft frequency. Its explicit expression as a function of angular misalignment, rotational speed and other joint parameters are given by reference [1] again. It may be noted that the motor speed is swept between 250 and 1500 revolutions per minute (rpm) for tests 2A and 2B, and only 850–1300 rpm for test 2C to seek out the exact resonance frequencies for modes 1 and 2. In each experiment, Φ_1 is again measured and used in the corresponding vibratory balance equation to compute the unknown modal damping coefficient of interest. The direct

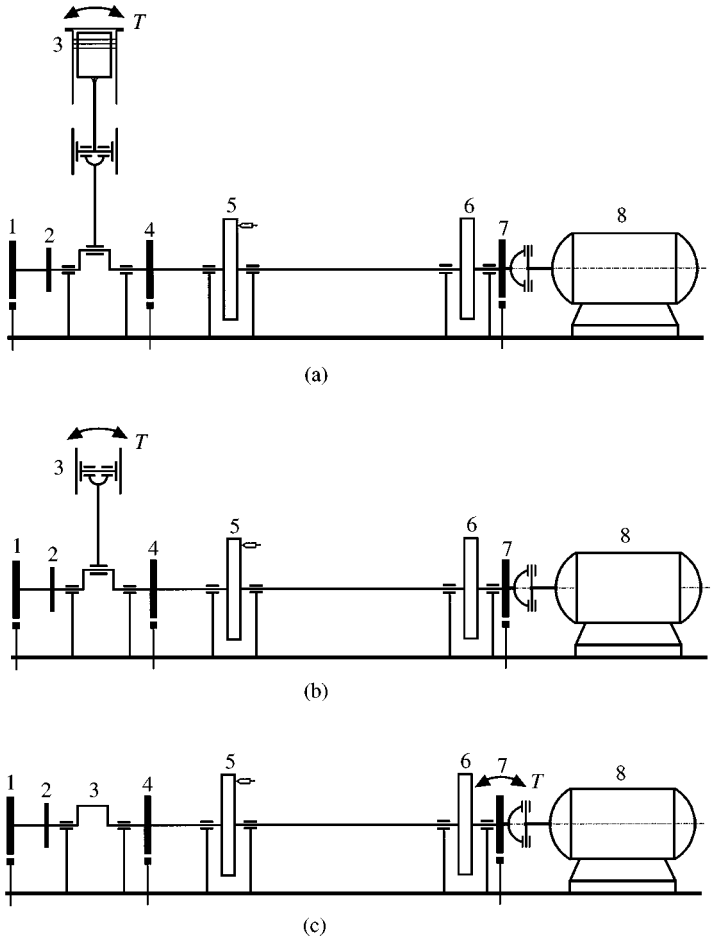

Figure 7. Proposed operating experiments for prediction of time-averaged modal damping coefficients of the single-cylinder engine of interest. Illustrated here are three different tests: (a) test 2A with complete engine installation; (b) test 2B with piston removed; (c) test 2C with crankshaft attached only. Lables: 1, measurement gear; 2, attachment disk; 3, cylinder; 4, measurement gear; 5, flywheel: 6 flywheel; 7, universal joint; 8, DC motor; (⊤), magnetic pickup transducer; (⇦), tachemeter; (T), input torque fluctuation.

calculation results of these operating experiments are shown in the second half of Table 2. The first half results in this table are computed from the quasi-stationary data applying equations (8–10). Recall that tests 1A and 2A yield the overall modal damping coefficient of the engine, tests 1B and 2B give the composite modal damping value without the piston damping effect, and tests 1C and 2C directly produce the time-averaged crankshaft damping coefficient. These results are used further to extract C_{ZP1} and the sum of $(C_{ZP2} + C_{ZR1} + C_{ZR2})$ as shown in Table 3. For the case of quasi-stationary analysis, we can also predict the time-averaged damping coefficients of the cross-head, and upper and lower pin joints in the connecting rods represented by C_{ZP2}, C_{ZR1} and C_{ZR2}, respectively, utilizing the data of Figure 6(b–d) in equation (10). It should be obvious that this decomposition cannot be achieved with solely operating data. Similar to the time-varying calculations, the time-averaged data also predicted relatively small damping contribution from the piston (less than 9% in all cases). The highest contributions are due to vibratory energy dissipations in the pin joints of the connecting rods and also the crankshaft/journal

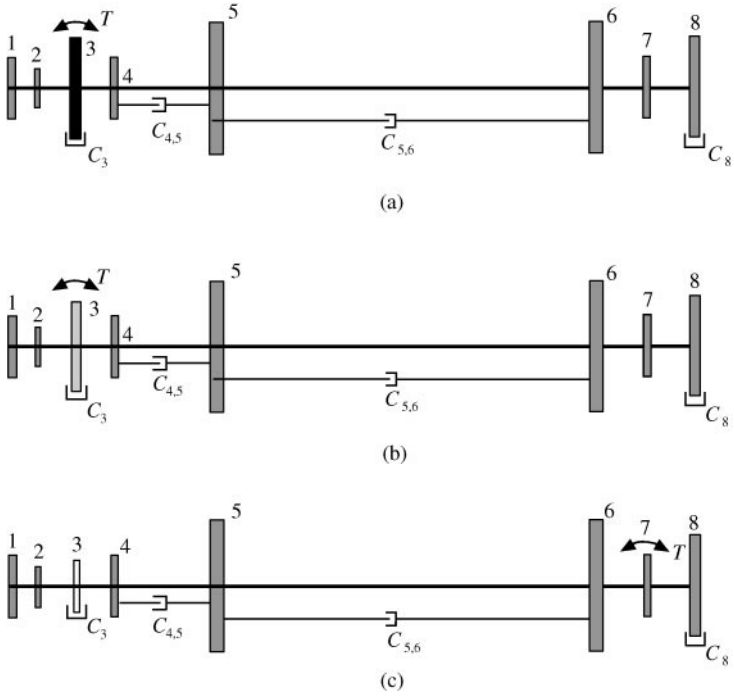

Figure 8. Lumped parameter torsional vibration models representing the proposed operating experiments for prediction of time-averaged modal damping coefficients: (a) complete powertrain torsional model, $T_3\Delta_3 = \omega_p\Phi_1[C_3\Delta_3^2 + C_8\Delta_8^2 + C_{4,5}(\Delta_4 - \Delta_5)^2 + C_{5,6}(\Delta_5 - \Delta_6)^2]$; (b) powertrain torsional model without piston component, $T_3\Delta_3 = \omega_p\Phi_1[C_3\Delta_3^2 + C_8\Delta_8^2 + C_{4,5}(\Delta_4 - \Delta_5)^2 + C_{5,6}(\Delta_5 - \Delta_6)^2]$; (c) powertrain torsional model with crankshaft attached only, $T_7\Delta_7 = \omega_p\Phi_1[C_3\Delta_3^2 + C_8\Delta_8^2 + C_{4,5}(\Delta_4 - \Delta_5)^2 + C_{5,6}(\Delta_5 - \Delta_6)^2]$.

TABLE 2

Predicted time-averaged modal damping coefficients of the complete and partially assembled engine components

Test condition	Test set-up	C_Z (N m s/rad)		$C_Z/I_3\omega_p$	
		Mode 1	Mode 2	Mode 1	Mode 2
Quasi-stationary	1A	0·9673	1·3162	0·0606	0·0307
	1B	0·8835	1·2262	0·0621	0·0318
	1C	0·3185	0·5828	0·0409	0·0258
Operating	2A	0·9401	1·3986	0·0588	0·0325
	2B	0·8635	1·2912	0·0607	0·0335
	2C	0·3021	0·5828	0·0388	0·0258

bearings; each accounts for about 30% of the overall modal damping level. As expected, the damping coefficients of mode 2 are higher than the fundamental mode in virtually all cases. Also in general, the comparison results in Tables 2 and 3 show excellent agreements between the quasi-stationary and operating experiments, which provide verification of the time-varying predictions.

TABLE 3

Comparison of time-averaged modal damping coefficients predicted by the quasi-stationary and operating experiments

Test condition	Engine components	Damping (N m s/rad)		Contribution (%)	
		Mode 1	Mode 2	Mode 1	Mode 2
Quasi-stationary (direct)	C_{ZP1} (piston)	0·0838	0·0900	8·66	6·84
	$C_{ZP2} + C_{ZR1} + C_{ZR2}$	0·5650	0·6434	58·41	48·88
	C_c (crankshaft)	0·3185	0·5828	32·93	44·28
Operating	C_{ZP1} (piston)	0·0766	0·1074	8·15	7·68
	$C_{ZP2} + C_{ZR1} + C_{ZR2}$	0·5614	0·7084	59·72	50·65
	C_c (crankshaft)	0·3021	0·5828	32·13	41·67
Quasi-stationary (least squares)	C_{ZP2}	0·0547	0·0546	5·65	4·15
	C_{ZR1}	0·2382	0·2864	24·63	21·76
	C_{ZR2}	0·2721	0·3024	28·13	22·97

4. CONCLUDING REMARKS

In this communication, we have successfully extended an earlier approach used only for predicting the overall torsional damping coefficient of a complete reciprocating engine to analyze the individual damping contributions from the numerous commonly known vibratory energy dissipation sources. The analysis yields a new set of analytical formulations to decompose the net connecting rod and crankshaft/journal bearings. A least-squares regression solution is also presented for separating the damping effects of the cross-head and pin joints in the connecting rod numerically. Coupled with the quasi-stationary and operating experiments of complete and partially assembled engine installations, both time-varying and time-averaged modal damping coefficients are obtained and correlated. The results reveal large damping contributions from the pin joints of the connecting rod and crankshaft/bearings, and the least vibratory energy dissipation effect from the friction between the piston and fixed cylinder bore.

REFERENCES

1. Y. WANG and T. C. LIM 2000 *Journal of Sound and Vibration* **238**, 710–719. Prediction of torsional damping coefficients in reciprocating engine.
2. J. P. DEN HARTOG 1985 *Mechanical Vibrations*. New York: Dover Publications.
3. W. KER WILSON 1963 *Practical Solution of Torsional Vibration Problems*. New York: John Wiley & Sons Inc.
4. J. F. SHANNON 1935 *Proceedings of the Institution of Mechanical Engineers* **131**, 387–435. Damping influences in torsional oscillation.
5. K. FEDERN and J. BROED 1982 *Motortechnische Zeitschrift* **43**, 525–529. Experimental analysis of torsional vibration damping in reciprocating engines.
6. P. DRAMINSKY 1948 *Proceedings of the Institution of Mechanical Engineers* **159**. Crank damping.
7. R. L. ESHLEMAN 1974 *Journal of Engineering for Industry* **96**, 441–449. Torsional resonance of internal combustion engines.
8. R. MACIOTTA and F. S. MERLINO 1965 *Proceedings of the 7th International Congress of Combustion Engines* (*7th CIMAC*). Recherchs sur d'amortissement des vibrations de torsiondans les installations avec moteurs diesel.

9. A. VALEV 1979 *Proceedings of the 13th International Congress of Combustion Engines (13th CIMAC)*. Relative motion between axis of pin and bore in connecting rod big-end bearings as the most essential damping cause for crankshaft torsional vibrations.
10. K. E. HAFNER 1977 *Hansa* **114**, 831–835. Einfluss der Gleitager auf die dampfung der torsionsschwingungen von kolbenmotoren.
11. S. IWAMOTO and K. WAKABAYASHI 1985 *Journal of the Marine Engineering Society* **20**, 776–781. A study on the damping characteristics of torsional vibration in diesel engines.